Micro-Raman investigation of optical phonons in ZnO nanocrystals

Khan A. Alim, Vladimir A. Fonoberov, Manu Shamsa, and Alexander A. Balandin[a)]
Nano-Device Laboratory, Department of Electrical Engineering, University of California-Riverside, Riverside, California 92521

(Received 28 February 2005; accepted 5 May 2005; published online 27 June 2005)

We have measured nonresonant and resonant Raman-scattering spectra from ZnO nanocrystals with an average diameter of 20 nm. Based on our experimental data and comparison with the recently developed theory, we show that the observed shifts of the polar optical-phonon peaks in the resonant Raman spectra are not related to the spatial phonon confinement. The very weak dispersion of the polar optical phonons in ZnO nanocrystals does not lead to any noticeable redshift of the phonon peaks for 20-nm nanocrystals. The observed phonon shifts have been attributed to the local heating effects. We have demonstrated that even the low-power ultraviolet laser excitation, required for the resonant Raman spectroscopy, can lead to the strong local heating of ZnO nanocrystals. The latter causes significant (up to 14 cm^{-1}) redshift of the optical-phonon peaks compared to their position in bulk crystals. Nonresonant Raman excitation does not produce noticeable local heating. The obtained results can be used for identification of the phonons in the Raman spectra of ZnO nanostructures. © *2005 American Institute of Physics*. [DOI: 10.1063/1.1944222]

I. INTRODUCTION

Zinc oxide (ZnO) presents interesting material system for investigation due to its wide band gap of 3.37 eV and some intriguing optical properties. A prominent feature of ZnO is its large exciton binding energy (~60 meV) at room temperature, which results in extreme stability of excitons.[1] Recently, nanostructures made of ZnO have attracted significant attention due to their proposed applications in the low-voltage and short-wavelength (368 nm) electro-optical devices, transparent ultraviolet (UV) protection films, gas sensors, and even spintronic devices. Despite practical importance, current knowledge of vibrational (phonon) properties of ZnO nanostructures is rather limited. Understanding the specifics of phonon spectrum (both optical and acoustic) of ZnO nanostructures can help in development of ZnO-based optoelectronic devices.

Raman spectroscopy is a nondestructive characterization method of choice for many recent studies of the vibrational properties of ZnO nanostructures.[2–14] Due to the Heisenberg uncertainty principal, the fundamental $q \sim 0$ Raman selection rule is relaxed for a finite-size domain, allowing the participation of phonons away from the Brillouin-zone center. The phonon uncertainty goes roughly as $\Delta q \sim 1/d$, where d is the diameter of a nanocrystal or quantum dot. This spatial confinement inside nanocrystals gives rise to a redshift and asymmetric broadening of the Raman peaks in nanostructures compared to bulk crystals.

ZnO is a semiconductor with wurtzite crystal structure. Wurtzite structure belongs to the space group $C_{6\nu}^4$ with two formula units per primitive cell, where all atoms occupy $C_{3\nu}$ sites. The Raman active zone-center optical phonons predicted by the group theory are $A_1+2E_2+E_1$. The phonons of A_1 and E_1 symmetry are polar phonons and, hence, exhibit different frequencies for the transverse-optical (TO) and longitudinal-optical (LO) phonons. Nonpolar phonon modes with symmetry E_2 have two frequencies, E_2(high) is associated with oxygen atoms and E_2(low) is associated with Zn sublattice. All described phonon modes have been reported in the Raman-scattering spectra of bulk ZnO.[15,16] Raman frequencies of both polar and nonpolar optical phonons are shifted in the spectra obtained from ZnO nanostructures compared to their positions in the spectra from bulk ZnO. The origin of these phonon frequency shifts is still under debate. In our recent letter,[17] we reported considerations, which brought us to the conclusion that the strong redshift of phonon peaks in Raman spectra from ZnO quantum dots and related nanostructures is related to local heating rather than to the spatial confinement. In order to avoid misinterpretation of the phonon properties of ZnO nanocrystals, it is important to gain complete understanding of the origin of the phonon frequency shifts. This paper provides details of our measurements and analysis in support of the local heating argument. It also outlines a method for distinguishing the confinement-induced shifts from the local heating shifts.

There are three possible mechanisms for the phonon peak shifts in Raman spectra of nanostructures. The first one is spatial confinement within the quantum dot (nanocrystal) boundaries. The second one is related to the phonon localization by defects. Nanocrystals or quantum dots, produced by chemical methods or by the molecular-beam epitaxy, normally have more defects than corresponding bulk crystals. The spatial confinement of optical phonons was studied by Richter *et al.*,[18] who showed that the Raman spectra of nanocrystalline semiconductors are redshifted and broadened due to the relaxation of the q-vector selection rule in the finite-size nanocrystals. Optical-phonon confinement in wurtzite nanocrystals leads to somewhat different changes in Raman spectra due to the optical anisotropy of wurtzite lattice. Recently, Fonoberov and Balandin[19–21] derived analytically an expression for the interface and confined polar optical-phonon modes in spheroidal quantum dots (QDs) with

[a)]Electronic mail: alexb@ee.ucr.edu

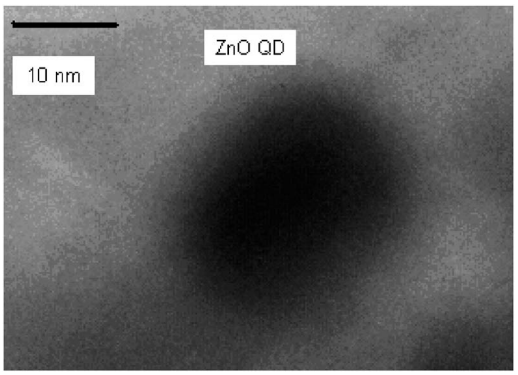

FIG. 1. TEM image of a ZnO nanocrystal. The nanocrystal shape is nearly spherical with the diameter of about 20 nm.

wurtzite crystal structure. Confined optical phonons in wurtzite nanocrystals were shown to have a discrete spectrum of frequencies different from those of bulk phonons.

In this paper we present details of the experimental study, which indicate that the large redshift (up to 14 cm^{-1}) in ZnO nanocrystals with the diameter of 20 nm is related to local heating rather than to phonon confinement. This conclusion is in line with several reports[22–35] of the photoluminescence (PL) and Raman peak shifts in nanostructures, which were also attributed due to the local laser heating. In Sec. II we describe the investigated ZnO nanocrystal samples. Section III provides details of the experimental procedure. Results and discussion are presented in Sec. IV. We give our conclusions in Sec. V.

II. SAMPLE DESCRIPTIONS

The samples used for the study are the powder of ZnO nanocrystals and the bulk ZnO reference sample. The bulk ZnO crystal (University Wafers) has wurtzite structure and dimensions of $5\times5\times0.5\ mm^3$ with the *a*-plane $(11\bar{2}0)$ facet. The investigated ZnO nanocrystals have been produced by the wet chemistry method. The average nanocrystal has almost spherical shape and a diameter of about 20 nm (see Fig. 1). The nanocrystals form a loose powder of white color. The air gaps, seen in Fig. 2, separate single nanocrystals and decrease the thermal conductivity of the sample. The chemical purity of the nanocrystal sample is 99.5%.

III. EXPERIMENTAL PROCEDURES

A high-resolution transmission electron microscope (TEM) FEI-PHILIPS CM 300 was used to investigate the size and shape of ZnO nanocrystals. A Renishaw micro-Raman spectrometer RM 2000 with visible (488 nm) and UV (325 nm) excitation lasers was employed to measure the nonresonant and resonant Raman spectra of ZnO samples, correspondingly. The number of gratings in the Raman spectrometer was 1800 for visible laser and 3000 for UV laser. All spectra were taken in the backscattering configuration at room temperature.

To observe the variation in LO peak position from bulk ZnO sample (polarized Raman), a rotation of the reference sample was performed from 0° to 360° angles in 45° intervals. To obtain the local temperature rise due to the nonresonant laser illumination, the laser power was varied from 3 to 15 mW. The corresponding local temperature was calculated from the comparison of the Stokes and anti-Stokes peaks in the Raman-scattering spectra. The UV laser power was varied from 0.2 to 20 mW in the resonant Raman-scattering experiments to investigate the dependence for optical-phonon peak position. The local temperature, in this case, was calculated theoretically.

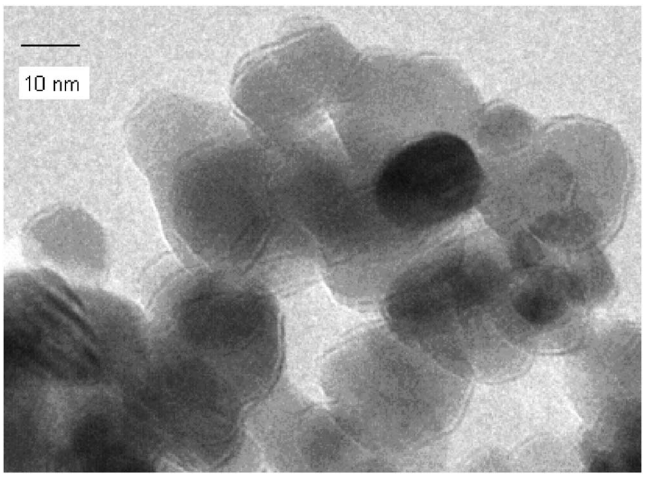

FIG. 2. TEM image of several ZnO nanocrystals. Air gaps in the loose powder of nanocrystals lead to the high thermal resistance and strong local laser heating.

IV. RESULTS AND DISCUSSION

The measured nonresonant Raman spectra of ZnO bulk and nanocrystals samples are shown in Figs. 3(a) and 3(b), respectively. The frequencies of the Raman active phonon modes reported previously for bulk ZnO are presented in Table I. All spectra in Fig. 3 were taken under the laser spot area of 1.6 μm^2 while the excitation laser power was kept at 15 mW. Comparing with the Table I, we can conclude that in the bulk ZnO spectrum the peak at 379 cm^{-1} corresponds to A_1(TO), 410 cm^{-1} corresponds to E_1(TO), and 439 cm^{-1} corresponds to E_2(high). No LO-phonon peaks are seen in the spectrum of bulk ZnO, because the incident light is perpendicular to the *c* axis of wurtzite ZnO. On the other hand, no TO phonons are observed in the nonresonant Raman spectrum of ZnO nanocrystals. In the nanocrystals spectrum, the peak at 436 cm^{-1} corresponds to E_2(high), which is shifted by 3 cm^{-1} compared to bulk. The peak at 582 cm^{-1} is positioned between A_1(LO) and E_1(LO) (see Table I), which is in a good agreement with the theoretical calculations of Fonoberov and Balandin.[19,21] The broad peak at about 330 cm^{-1} seen in both spectra in Fig. 3 is attributed to the second-order Raman processes.

Since the nanocrystal size is relatively large, the observed redshift of the E_2(high) phonon cannot be ascribed to the optical-phonon confinement by the nanocrystal boundaries. In order to investigate the factors contributing to the E_2(high) phonon peak shift, we carried out a set of experiments. Under visible (488 nm) excitation, the variation in the laser power does not produce any change in E_2(high) phonon peak position. In addition, we have estimated the local tem-

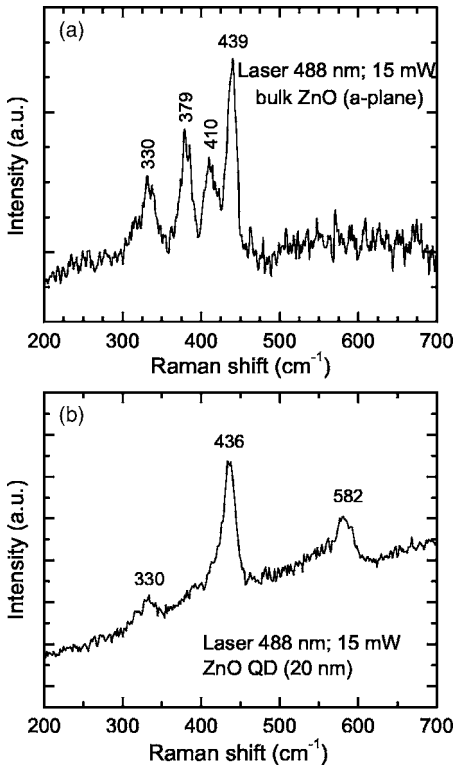

FIG. 3. Nonresonant Raman spectra for (a) bulk ZnO *a* plane; (b) for ZnO nanocrystals. Photoluminescence background is subtracted from the bulk ZnO spectrum.

perature rise due to the laser heating using the relationship $I_S/I_{AS} \approx \exp[\hbar\omega/k_BT]$, where I_S and I_{AS} are the intensities of the Stokes and anti-Stokes peaks, respectively, and T is the local absolute temperature. The laser power and the corresponding calculated temperatures are given in Table II. Raman spectrum of ZnO nanocrystals, which have been used to measure the local temperature, is shown in Fig. 4. Since the change of the visible laser power does not lead to any changes in the E_2(high) phonon frequency, and the local temperature calculated for the maximum laser power is less than 50 °C, it is clear that local heating cannot be responsible for E_2(high) phonon peak shift in the nonresonant Raman spectra. At the same time, it is known that the E_2(high) phonon in ZnO can exhibit a large variation of the frequency when either the isotopic masses of atoms constituting ZnO are changed or the homogeneously distributed impurities are present.[36] Therefore, the likely explanation of the E_2(high) phonon peak shift is the presence of 0.5% impurities of Cu, Mn, or Pd in the ZnO nanocrystals sample.

The obtained resonant Raman-scattering spectra of bulk ZnO and ZnO nanocrystals are shown in Figs. 5(a) and 5(b). The spectrum of bulk ZnO was taken at the laser power of 20 mW and the laser spot size of 1.6 μm^2. The spectrum of

TABLE I. Raman active phonon mode frequencies (in cm^{-1}) for bulk ZnO. Presented data are a compilation of the results different studies reported in Ref. 15.

E_2(low)	A_1(TO)	E_1(TO)	E_2(high)	A_1(LO)	E_1(LO)
102	379	410	439	574	591

TABLE II. Estimated temperature at different laser power levels in the case of visible excitation.

Power (mW)	I_S/I_{AS}	Temperature
3.75	7.857	304.12 K
7.5	7.383	312.73 K
15	7.016	322.73 K

ZnO nanocrystals was taken at the 5-mW laser power and the laser spot size of 1.6 μm^2. A noticeable difference between the resonant and nonresonant Raman spectra is that a number of LO multiphonon peaks and no TO phonons are observed under the resonant excitation. In the bulk ZnO spectrum, a 574-cm^{-1} peak corresponds to A_1(LO) phonon mode (see Table I) while the other peaks are just higher-order peaks of LO phonons. The 1LO-phonon peak of ZnO varies[16] by several cm^{-1} because of the anisotropic short-range forces in the uniaxial ZnO lattice. The peak varies from 591 cm^{-1} for polarization field $\boldsymbol{\xi} \perp c$ to 574 cm^{-1} for $\boldsymbol{\xi} \| c$, where c is the optical axis. To clarify this, we took the polarized Raman spectra of bulk ZnO sample while rotating it around the z axis (corresponds to the laser light direction). The position of the 1LO peak as a function of the angle θ is shown in Table III. The results are in excellent agreement with Ref. 16.

Since the size of ZnO nanocrystals is relatively large, the 1LO-phonon frequency should be between 574 and 591 cm^{-1}. But, in the nanocrystals Raman spectrum, the 1LO peak appears at 564 cm^{-1}, which indicates a redshift of more than 10 cm^{-1}. The observed huge redshift could hardly be attributed to the intrinsic impurity or defects in the sample. The only possible reason for the observed redshift is intense local heating induced by UV laser in the powder of ZnO nanocrystals.[17,37] To verify this assumption, we varied the UV laser power as well as the area of the illuminated laser spot on the ZnO nanocrystal sample and recorded the corresponding Raman spectra.

The obtained Raman spectra under different laser power with the laser spot areas of 11 and 1.6 μm^2 are shown in Figs. 6 and 7, correspondingly. In both Figs. 6 and 7, the 1LO frequency was plotted as a function of laser power in the insets. One can see from Fig. 6 that the redshift of the

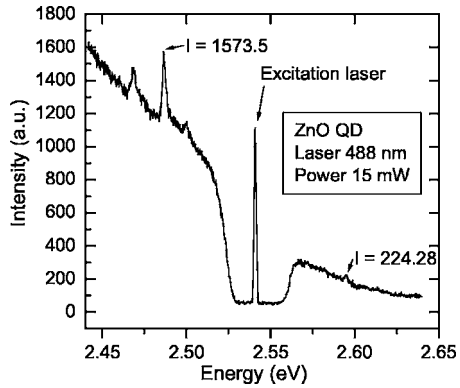

FIG. 4. Raman spectrum of ZnO nanocrystals used to measure the local temperature. Laser power is 15 mW. Intensities of the Stokes (1573.5) and anti-Stokes (224.28) peaks are shown in arbitrary units.

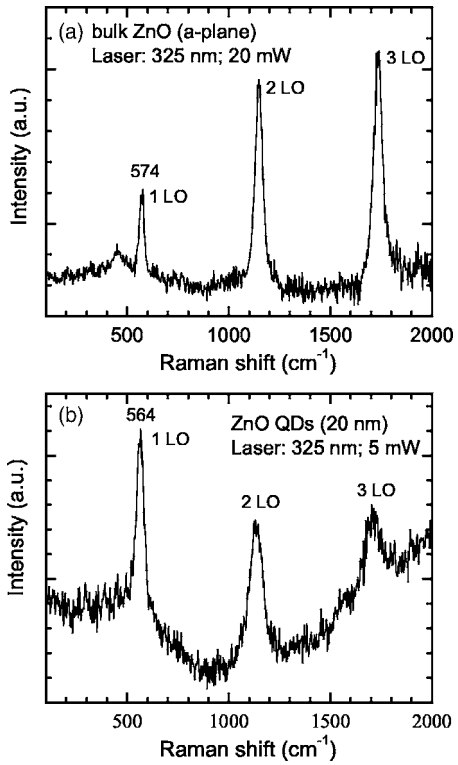

FIG. 5. Resonant Raman spectra of (a) bulk ZnO (*a* plane) and (b) ZnO QDs (20 nm). Photoluminescence background is subtracted from the bulk ZnO spectrum.

LO-phonon peak in the ZnO nanocrystals increases almost linearly with the laser power and reaches 10 cm^{-1} for the laser power of 20 mW. It is observed from Fig. 7 that at the smaller illuminated laser spot of 1.6 μm^2, the redshift of the LO-phonon frequency for ZnO nanocrystals increases at a faster rate. In the latter case, the LO peak redshift reaches about 14 cm^{-1} for the laser power of only 10 mW. The 0.2-mW laser power was too small to detect the spectrum when the laser spot was 11 μm^2 and the 20-mW laser power was too high when the laser spot was 1.6 μm^2. All reported spectra were taken with the same accumulation time of 60 s. The attempts to record the LO-phonon frequency using the illuminated spot of area 1.6 μm^2 and UV laser power of 20 mW resulted in the thermal destruction of ZnO nanocrystals in the illuminated spot. The destruction or significant change in the morphology of nanocrystals was confirmed by the absence of any ZnO nanocrystals peak from the same spot at any laser power once the 20-mW power had been used.

It is known that bulk ZnO semiconductor sublimes at 1800 °C and melts at 2200 °C temperature. At the same time, ZnO nanocrystal powder evaporates at significantly lower (1380 °C) temperature.[38] The density of the reference bulk ZnO crystal is 5.6 g/cm^3 while the density of the nanocrystal power is 0.3–0.45 g/cm^3. The latter together with the TEM data indicate that there is large amount of air in the gaps between nanocrystals. As a result, the thermal conductivity of the nanocrystal sample is drastically reduced. We argue that the reduced thermal conductivity of the ZnO nanocrystals and correspondingly increased local heating explain the appearance of such a large redshift in the Raman spectra of ZnO nanocrystals. This observation can be important for nanocrystals made of other material systems (there is a body of literature with claims of significant redshifts for nanocrystals with relatively large diameters).

TABLE III. Polarized Raman LO peak position for ZnO bulk (*a* plane) as a function of the angle θ.

θ	0°	45°	90°	135°
1LO	579 cm^{-1}	574 cm^{-1}	580 cm^{-1}	583 cm^{-1}
θ	180°	225°	270°	315°
1LO	579 cm^{-1}	577 cm^{-1}	579 cm^{-1}	584 cm^{-1}

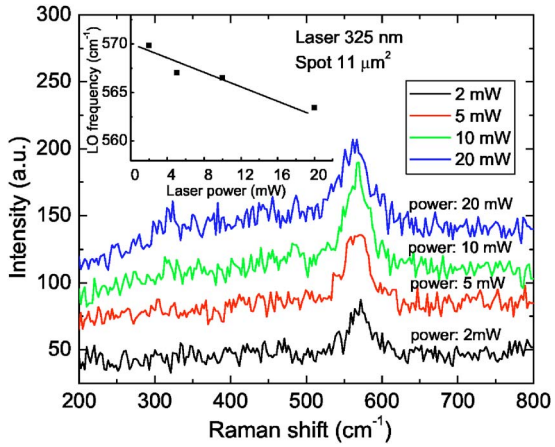

FIG. 6. (Color online) Raman spectra of ZnO QD at illumination spot of 11 μm^2 and different laser powers.

The temperature dependence of the Raman scattering has been investigated in details for different materials (e.g., Si, Ge, GaN, etc.).[22–35] The Raman shift dependence on temperature can be written as a function of two additive effects: the change in the vibration frequencies due to the thermal expansion (volume change) and the change due to anharmonic coupling of phonons. Taking into account the thermal expansion and the anharmonic coupling effects, the LO-phonon frequency can be written as[39]

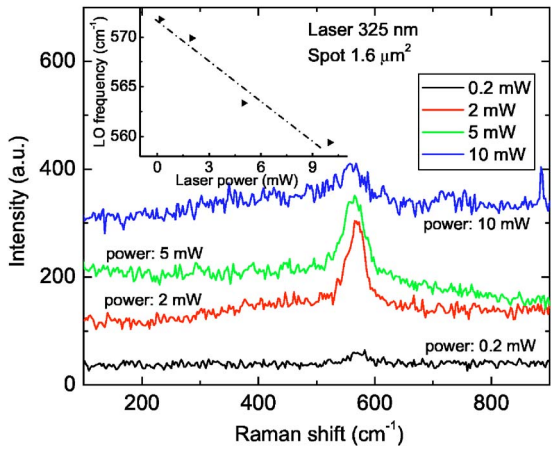

FIG. 7. (Color online) Raman spectra of ZnO QDs at illuminated spot of 1.6 μm^2 and different laser powers.

$$\omega(T) = \exp\left[-\gamma\int_0^T \{2\alpha_\perp(T') + \alpha_\parallel(T')\}dT'\right] \times(\omega_0 - M_1 - M_2) + M_1\left[1 + \frac{2}{e^{\hbar\omega_0/2k_BT} - 1}\right] + M_2\left[1 + \frac{3}{e^{\hbar\omega_0/3k_BT} - 1} + \frac{3}{(e^{\hbar\omega_0/3k_BT} - 1)^2}\right], \quad (1)$$

where the Grüneisen parameter of the LO phonon in ZnO $\gamma=1.4$,[40] the thermal expansion coefficients $\alpha_\perp(T)$ and $\alpha_\parallel(T)$ for ZnO are taken from Ref. 41, and the anharmonicity parameters M_1 and M_2 are assumed to be equal to those of the A_1(LO) phonons from Ref. 39, i.e., $M_1=-4.14$ cm^{-1} and $M_2=-0.08$ cm^{-1}. Fitting the experimental data shown in Fig. 7 (area=1.6 μm^2) with Eq. (1), we established that the observed 14-cm^{-1} redshift shown in Fig. 7, indeed, corresponds to the ZnO temperature of about 700 °C. If we assume that the temperature rise in ZnO nanocrystals is proportional to the UV laser power, the observed 14-cm^{-1} LO redshift corresponds to the local temperature of 700 °C when the illuminate spot is 1.6 μm^2 and the laser power is 10 mW. Therefore, the 20-mW laser power leads to the local temperature rise up to about 1400 °C at the illuminated spot, which causes the destruction or significant changes in the morphology of ZnO nanocrystals.

V. CONCLUSION

In conclusion, intense local heating caused by the UV laser in resonant Raman-scattering measurements strongly affects the spectra of ZnO QDs. By varying laser power, we observed that nonresonant Raman scattering does not cause strong local heating, as well as no redshift is observed. We have claimed here that intrinsic defects in QD sample can introduce shifts of only few cm^{-1} in E_2(high) phonon peak, but a small UV laser power can lead to strong local heating and to a large redshift of the LO-phonon frequency. The common laser power that is used to measure Raman spectra of bulk ZnO, can cause the destruction of ZnO QD ensembles, if the illuminated spot is small. The results presented in this paper are important to take into account when measuring Raman scattering of ZnO QDs.

ACKNOWLEDGMENTS

The authors acknowledge the financial and program support of the DARPA-SRC Microelectronics Advanced Research Corporation (MARCO) and its Focus Center on Functional Engineered Nano Architectonics (FENA). The work was supported in part through ONR Young Investigator Award to one of the authors (A.A.B).

[1] Y. Chen, D. M. Bagnall, H. Koh, K. Park, K. Hiraga, Z. Zhu, and T. Yao, J. Appl. Phys. **84**, 3912 (1998).
[2] X. T. Zhang *et al.*, J. Phys. D **34**, 3430 (2001).
[3] C. Bundesmann, N. Ashkenov, M. Schubert, D. Spemann, T. Butz, E. M. Kaidashev, M. Lorenz, and M. Grundmann, Appl. Phys. Lett. **83**, 1974 (2003).
[4] A. Kaschner *et al.*, Appl. Phys. Lett. **80**, 1909 (2002).
[5] H. T. Ng, B. Chen, J. Li, J. Han, M. Meyyappan, J. Wu, S. X. Li, and E. E. Haller, Appl. Phys. Lett. **82**, 2023 (2003).
[6] X. Wang, Q. Li, Z. Liu, J. Zhang, Z. Liu, and R. Wang, Appl. Phys. Lett. **84**, 4941 (2004).
[7] C. Geng, Y. Jiang, Y. Yao, X. Meng, J. A. Zapien, C. S. Lee, Y. Lifshitz, and S. T. Lee, Adv. Funct. Mater. **14**, 589 (2004).
[8] R. P. Wang, G. Xu, and P. Jin, Phys. Rev. B **69**, 113303 (2004).
[9] Y. J. Xing *et al.*, Appl. Phys. Lett. **83**, 1689 (2003).
[10] C. Xu, G. Xu, Y. Liu, and G. Wang, Solid State Commun. **122**, 175 (2002).
[11] X. H. Zhang, S. Y. Xie, Z. Y. Jiang, X. Zhang, Z. Q. Tian, Z. H. Xie, R. B. Huang, and L. S. Zheng, J. Phys. Chem. B **107**, 10114 (2003).
[12] M. Rajalakshmi, A. K. Arora, B. S. Bendre, and S. Mahamuni, J. Appl. Phys. **87**, 2445 (2000).
[13] H. Zhou, H. Alves, D. M. Hofmann, W. Kriegseis, B. K. Meyer, G. Kaczmarczyk, and A. Hoffmann, Appl. Phys. Lett. **80**, 210 (2002).
[14] Z. Wang, H. Zhang, L. Zhang, J. Yuan, S. Yan, and C. Wang, Nanotechnology **14**, 11 (2003).
[15] N. Ashkenov *et al.*, J. Appl. Phys. **93**, 126 (2003).
[16] J. F. Scott, Phys. Rev. B **2**, 1209 (1970).
[17] K. A. Alim, V. A. Fonoberov, and A. A. Balandin, Appl. Phys. Lett. **86**, 053103 (2005).
[18] H. Richter, Z. P. Wang, and L. Ley, Solid State Commun. **39**, 625 (1981).
[19] V. A. Fonoberov and A. A. Balandin, Phys. Rev. B **70**, 233205 (2004).
[20] V. A. Fonoberov and A. A. Balandin, Phys. Status Solidi C **1**, 2650 (2004).
[21] V. A. Fonoberov and A. A. Balandin, J. Phys.: Condens. Matter **17**, 1085 (2005).
[22] P. G. Klemens, Phys. Rev. **148**, 845 (1966).
[23] T. R. Hart, R. L. Aggarwal, and B. Lax, Phys. Rev. B **1**, 638 (1970).
[24] H. W. Lo and A. Compaan, J. Appl. Phys. **51**, 1565 (1980).
[25] R. Tsu and J. G. Hernandez, Appl. Phys. Lett. **41**, 1016 (1982).
[26] M. Balkanski, R. F. Wallis, and E. Haro, Phys. Rev. B **28**, 1928 (1983).
[27] J. Menendez and M. Cardona, Phys. Rev. B **29**, 2051 (1984).
[28] S. Piscanec, M. Cantoro, A. C. Ferrari, J. A. Zapien, Y. Lifshitz, S. T. Lee, S. Hofmann, and J. Robertson, Phys. Rev. B **68**, 241312 (2003).
[29] R. S. Krishnan, Proc. Indian Acad. Sci., Sect. A **24**, 45 (1946).
[30] E. Anatassakis, H. C. Hwang, and C. H. Perry, Phys. Rev. B **4**, 2493 (1971).
[31] W. J. Borer, S. S. Mitra, and K. V. Namjoshi, Solid State Commun. **9**, 1377 (1971).
[32] R. A. Cowley, J. Phys. (Paris) **26**, 659 (1965).
[33] A. Temple and C. E. Hathaway, Phys. Rev. B **7**, 3685 (1973).
[34] F. Cerdeira and M. Cardona, Phys. Rev. B **5**, 1440 (1972).
[35] J. H. Jung, Solid State Commun. **133**, 103 (2004).
[36] J. Serrano, F. J. Manjon, A. H. Romero, F. Widulle, R. Lauck, and M. Cardona, Phys. Rev. Lett. **90**, 055510 (2003).
[37] L. Bergman, X. B. Chen, J. L. Morrison, J. Huso, and A. P. Purdy, J. Appl. Phys. **96**, 675 (2004).
[38] K. Park, J. S. Lee, M. Y. Sung, and S. Kim, Jpn. J. Appl. Phys., Part 1 **41**, 7317 (2002).
[39] W. S. Li, Z. X. Shen, Z. C. Feng, and S. J. Chua, J. Appl. Phys. **87**, 3332 (2000).
[40] F. Decremps, J. Pellicer-Porres, A. M. Saitta, J. C. Chervin, and A. Polian, Phys. Rev. B **65**, 092101 (2002).
[41] H. Iwanaga, A. Kunishige, and S. Takeuchi, J. Mater. Sci. **35**, 2451 (2000).